

# Swept-Tone Stimulus-Frequency Otoacoustic Emissions in Human Newborns

Trends in Hearing  
Volume 23: 1–15  
© The Author(s) 2019  
Article reuse guidelines:  
sagepub.com/journals-permissions  
DOI: 10.1177/2331216519889226  
journals.sagepub.com/home/tia  


Carolina Abdala<sup>1</sup> , Ping Luo<sup>1</sup>, and Yeini Guardia<sup>1</sup>

## Abstract

Several types of otoacoustic emissions have been characterized in newborns to study the maturational status of the cochlea at birth and to develop effective tests of hearing. The stimulus-frequency otoacoustic emission (SFOAE), a reflection-type emission elicited with a single low-level pure tone, is the least studied of these emissions and has not been comprehensively characterized in human newborns. The SFOAE has been linked to cochlear tuning and is sensitive to disruptions in cochlear gain (i.e., hearing loss) in adult subjects. In this study, we characterize SFOAEs evoked with rapidly sweeping tones in human neonates and consider the implications of our findings for human cochlear maturation. SFOAEs were measured in 29 term newborns within 72 hr of birth using swept tones presented at 2 oct/s across a four-octave frequency range (0.5–8 kHz); 20 normal-hearing young adults served as a control group. The prevalence of SFOAEs in newborns was as high as 90% (depending on how response “presence” was defined). Evidence of probe-tip leakage and abnormal ear-canal energy reflectance was observed in those ears with absent or unmeasurable SFOAEs. Results in the group of newborns with present stimulus-frequency emissions indicate that neonatal swept-tone SFOAEs are adult-like in morphology but have slightly higher amplitude compared with adults and longer SFOAE group delays. The origin of these nonadult-like features is probably mixed, including contributions from both conductive (ear canal and middle ear) and cochlear immaturities.

## Keywords

cochlea, otoacoustic emissions, neonate, development, chirps

Date received: 19 July 2019; revised: 16 October 2019; accepted: 24 October 2019

## Introduction

The stimulus-frequency otoacoustic emission (SFOAE), evoked by a single low-level pure tone, is a reflection-source otoacoustic emission (OAE). The generation mechanisms of reflection- and distortion-source OAEs are distinct: The SFOAE arises as reflections off of natural (or pathological) micromechanical irregularities occurring in tissue along the cochlear spiral. These reflections are strongest near the peak of the traveling wave (Zweig & Shera, 1995) and so these emissions are thought to be good indicators of cochlear gain and sharp tuning, also coded at the peak of the wave. When the traveling wave peak is reduced or broadened (which we understand to happen when sensory hearing loss is present), the strength of intracochlear reflections is also reduced. Hence, SFOAE presence and amplitude serve as indicators of hearing loss. Reflection-source OAEs are more sensitive to slight-mild amounts of hearing loss

than OAEs evoked by nonlinear distortion, most notably at low to mid frequencies (Abdala & Kalluri, 2017; Gorga et al., 1993a, 1993b; Lapsley Miller, Marshall, & Heller, 2004; Lapsley Miller, Marshall, Heller, & Hughes, 2006), and have shown accuracy in the detection of adult hearing loss comparable to that achieved by more commonly studied emissions, for example, transient-evoked OAEs and distortion-product OAEs (DPOAEs; Ellison & Keefe, 2005).

<sup>1</sup>Caruso Department of Otolaryngology, Auditory Research Center, Keck School of Medicine, University of Southern California, Los Angeles, CA, USA

### Corresponding Author:

Carolina Abdala, Caruso Department of Otolaryngology, Auditory Research Center, Keck School of Medicine, University of Southern California, 1640 Marengo St., Ste. #326, Los Angeles, CA 90033, USA.  
Email: carolina.abdala@usc.edu



SFOAEs have not been studied comprehensively in neonatal ears; however, a preliminary study from our laboratory recorded discrete-tone SFOAEs in a small group of newborns over a restricted frequency range: approximately 1.3 to 2 kHz. We found that infants had SFOAEs with higher amplitudes than adults in this narrow range of frequencies and longer group delays, possibly due to middle-ear (vs. cochlear) immaturities. Unlike discrete tones, rapidly sweeping tones allow for the efficient presentation of stimuli across a wide frequency range and provide the opportunity for fine-resolution data analysis. The speed and efficiency of the swept-tone method allow for the averaging of hundreds of sweeps (Abdala, Luo, & Shera, 2015; Kalluri & Shera, 2013), which are crucial to reduce the elevated noise floors typical in neonatal measures. This study seeks to characterize fine-resolution SFOAEs evoked with sweeping tones in newborns across a broad frequency range and to further our understanding of the developmental status of the human cochlea at birth.

SFOAEs offer a window into the developmental status of cochlear tuning and gain in newborns. Much work on human cochlear development has been conducted by studying the separated reflection component of the DPOAE as a gauge of cochlear mechanics. The DPOAE is comprised of two components: the typically dominant distortion component, which is generated by cochlear nonlinearities near the cochlear site corresponding to the stimulus frequency,  $f_2$  and an often smaller reflection component generated by intracochlear reflections at the  $2f_1 - f_2$  place. The reflection component of the DPOAE is larger in newborns than adults (suggesting greater contribution from intracochlear reflections to the DPOAE in newborn ears) and has longer delays (Abdala & Dhar, 2012). It is likely that multiple factors contributed to these findings as will be further considered in the “Discussion” section. However, the reflection component of the DPOAE is not an ideal tool for studying human cochlear maturation: It must first be separated from the total DPOAE using one of a variety of signal processing techniques, none of which is perfect; the strength of the signal evoking the reflection part of the DPOAE cannot be well quantified (because it is the forward-going component of the distortion wave); and the reflection component of the DPOAE is typically low amplitude, making it difficult to measure and characterize well (see Abdala, Guardia, & Shera, 2018). The SFOAE provides a more direct and nonconfounded measure of intracochlear reflections. It has recently been characterized in normal-hearing young adults (Abdala, Guardia, et al., 2018; Dewey & Dhar, 2017; Mishra & Talmadge, 2018) and older adults (Abdala, Ortmann, & Shera, 2018), and the optimal testing parameters and strategies have been well defined. Characterizing the swept-tone SFOAE in newborns

adds converging data to the existing literature available on functional status of the human cochlea at birth and disentangles previous methodological confounds that used less direct measures.

## Methods

### Subjects

Thirty-two healthy term newborns born at the Los Angeles County + University of Southern California Hospital were recruited within 72 hr of birth. Three of these prospective subjects exhibited excessive movement and restlessness which precluded testing; hence, 29 newborns were included in the initial subject pool. All newborns passed the hospital hearing screening conducted with a click-evoked (35 dB HL) auditory brainstem response. Neonates were born between 35 and 41 gestational weeks and tested at a mean postconceptional age of 38 weeks. Their average birthweight was 3,079 g and their average 1 and 5 min Apgar scores (which are scores summarizing the health of neonates at birth) were 8 and 9, respectively, out of a possible 10. After obtaining parental consent, the newborns were wheeled in an open isolette to the Infant Auditory Research Laboratory within the Neonatology unit of the hospital for testing. The newborns were swaddled securely, comforted and calmed, and then transferred to a closed Neonatal Intensive Care Unit-type isolette once asleep; a closed isolette (such as those used in the Neonatal Intensive Care Unit) was utilized for data collection to partially attenuate ambient sound.

Twenty young adult subjects (11 females and 9 males) ranging from 22 to 28 years old (mean 25.3 years) served as a control group. SFOAEs from adult subjects were not fully described or characterized in this study because other publications from our laboratory and others' have provided characterization of SFOAEs in human adults. Here, the adults served as a normative referent only. Twelve right ears and eight left ears were tested. Adult subjects had no history of otologic disease, hearing loss, or chronic noise exposure. All had normal otoscopic exams and Type-A tympanograms (226-Hz probe tone) with peaks between  $\pm 50$  daPa. Audiometric thresholds were  $\leq 15$  dB HL for frequencies tested at one-octave intervals between 500 and 8000 Hz.

### Hardware and Calibration

A BabyFace Pro USB High Speed Audio Interface (RME Audio, Germany) and ER-10X probe system (Etymotic Research, Elk Grove Village, IL) controlled by custom software written in MATLAB (Mathworks, Natick, MA) were used to generate stimulus waveforms and record SFOAEs. Microphone voltages were

amplified (+20 dB) and high-pass filtered (300-Hz cutoff frequency) before A/D conversion.

For infants, either a pliable red silicone probe tip (4 mm) or a modified yellow silicone tip (3 mm) was fitted snugly on an ER-10X probe assembly and placed into the ear-canal meatus. This study was our first study using the advanced Etymotic-Research 10X probe microphone with human newborns (and to our knowledge no other report of its use with this population exists in the literature). The probe cable was fed through the open side port of the isolette and suspended with a hook adhered to the wall of the unit. Care was taken to avoid contact between the cable and the isolette or the swaddling blankets. For adults, OAE testing was performed within a double-walled, sound-attenuated chamber (IAC: Industrial Acoustics Co.) with the subject reclining in an ergonomic chair. The probe cable was suspended from the ceiling by a hook, and the probe tip was carefully positioned into the ear canal and secured with a nylon headband. No part of the cable came in contact with the subject or the test chair. Subjects rested quietly or watched a subtitled video during testing.

We used a conventional, in-the-ear method of stimulus calibration where the target stimulus level was measured as the total ear canal sound pressure level (SPL) at the microphone. To do this, we fitted the ER-10X probe into the ear canal of each subject and presented a series of moderate-level chirps. At any given frequency, the stimulus calibration function specified the complex-valued total pressure produced at the probe microphone when a sinusoid of amplitude 1 V was presented to the earphone. The function was then used to determine the driving voltage needed to achieve target SPL across frequency in each ear. The calibration was repeated (and stimulus levels updated) every 5 to 6 min throughout data collection and whenever the probe was refit (due to shifting or movement). The calibration function provided other valuable information as well: the ear-canal SPL across frequency (which allowed us to detect leaks in the probe seal), the depth of the probe fit (by the location of the half-wave resonance peak), and ear-canal pressure reflectance, which allowed us to calculate wideband energy reflectance as an indicator of probe fit and middle-ear status.

### Protocol

The protocol used for this study was reviewed and approved by the institutional review board of the University of Southern California (Approval # HS-15-00341). Two testers worked together to collect newborn data; one implemented the program software (Tester), while the other was responsible for fitting the probe, observing and calming the baby, and ensuring that the probe fit remained in place (Baby Monitor).

If the baby became restless or the probe shifted during testing, the Baby Monitor communicated this to the Tester who paused data collection thus allowing the Baby Monitor to remediate the situation. At the beginning of a test session, the probe was fit in the newborn ear and calibration was performed. Our pilot work had indicated that the large ER-10X probe did not conform naturally to the small and flaccid newborn ear canal and was difficult to fit in this age-group; hence, we used several indicators to ensure an adequate fit before recording SFOAEs: (a) ear-canal pressure reflectance had to be  $<1$  for frequencies between 0.5 and 8 kHz; (b) the SPL versus frequency function had to show a relatively flat levels between 0.25 and 2 kHz, indicating the absence of a leak and suggesting a firm seal between the probe and the ear canal; (c) the half-wave resonance peak frequency had to approximate typical neonatal values ( $\sim 9600$  Hz); and (d) an abbreviated DPOAE test ( $f_2 = 1$  to 4 kHz; 48 sweeps at 2 oct/s) had to indicate a present DPOAE, consistent with a clear ear canal and an adequate probe fit. If the reflectance was abnormal ( $>1$ ), a leak was detected, there was excessive noise, or the DPOAE was not present, the baby was calmed and the probe was refit. Before commencing the SFOAE protocol, this sequence was often repeated multiple times until a probe fit was deemed to be adequate as per the screening indicators.

SFOAEs were evoked by 40 dB SPL pure tones swept logarithmically in a downward direction at 2 oct/s from  $f_2 = 0.5$  to 8 kHz for both newborn and adult subjects. Four-frequency segments, each roughly one-octave wide, were stacked and presented concurrently for rapid data collection (see Abdala, Guardia, et al., 2018). A suppressor tone at 55 dB SPL was simultaneously presented at a frequency ratio of 0.95 (re: probe) and a modified interleaved suppression paradigm was utilized to extract SFOAEs (Shera & Guinan, 1999). Past work studying the maturation of cochlear nonlinearity and two-tone suppression in human newborns suggests that these properties are mature by term birth (Abdala, 1998, 2000; Abdala & Keefe, 2006; Abdala, Keefe, & Oba, 2007). For this reason, we applied the same suppressor level for newborns and adults to extract the SFOAE. Responses to four stimulus combinations were measured:  $p_1$  = probe tone alone,  $p_2$  = probe and suppressor tone (+polarity),  $p_3$  = probe tone alone, and  $p_4$  = probe and suppressor tone (-polarity). The SFOAE time waveform was extracted using the formula:  $p_{\text{SFOAE}} = (p_1 + p_3 - p_2 - p_4)/2$ . Pilot testing determined that between 266 and 512 sweeps contributing to the average would provide adequate signal-to-noise ratio (SNR) in newborns; 128 sweeps contributed to the averaged SFOAE in adult subjects. Seven of the newborns also provided SFOAE data at a probe level of 20 dB SPL (suppressor level = 55 dB SPL).

### Real-Time Glitch Detection and Post Hoc Artifact Rejection

During data collection, each SFOAE time waveform was analyzed in the frequency domain using least-squares fitting (LSF) techniques (see the following section for details about the LSF method); hence, the median magnitude of the SFOAE was calculated and updated with each new sweep. A glitch was detected as a data point differing by more than two standard deviations (*SDs*) from the ongoing median SFOAE spectrum; when present, a glitch triggered an additional sweep. Data collection stopped when all points across frequency had accrued the target number of glitch-free sweeps. Meeting this accrual goal typically required 15% to 20% additional sweeps (beyond the target number) due to artifacts.

The rejection of artifacts was performed off-line. Artifacts were identified as individual frequency points whose magnitude exceeded five *SDs* ( $\sim 11.5$  dB in newborns) from the final SFOAE median amplitude. Note that the post hoc rejection criterion was stricter than the criteria applied for detection of a glitch during testing. Online detection served the sole purpose of triggering additional sweeps so as to have enough data for a robust average after 15% to 20% (on average) of the data points were rejected off-line. The five *SD* rejection criteria were determined by assessing the effect of point rejection on the OAE SNR. Once identified, artifactual points in the spectra were linked back to the corresponding point in the time waveform and a segment centered on the artifact frequency and equal to 20% of the analysis window ( $\pm 10\%$  on either side) was eliminated.

### SFOAE Estimates

SFOAEs were analyzed from the recorded ear-canal signals using an LSF technique applied to the time waveform (Abdala et al., 2015; Kalluri & Shera, 2013; Long, Talmadge, & Lee, 2008). Briefly, the OAE time waveform is segmented into moving analysis windows that shift in 0.01 octave steps. Models for the suppressor and SFOAE are created and the amplitude and phase of the signals of interest within each analysis window are then estimated by minimizing the sum of the squared residuals between the model and the data to achieve the best fit. The LSF model was applied at 100 points per octave resulting in OAE spectra consisting of approximately 400 points across the four-octave test range. The noise floor at each frequency was estimated by averaging the four LSF spectral levels computed at frequencies closest to the OAE. These frequencies were 1.10, 1.12, 1.14, and 1.16 times the SFOAE frequency. The LSF procedure employs analysis bandwidths (i.e., window durations) that vary continuously as a function of frequency with

the goal of keeping constant the number of cycles of phase rotation in each analysis window. To achieve this, the LSF analysis bandwidth shifted from 0.16 (at 500 Hz) to 0.05 ms (at 8 kHz). Parametric studies from our laboratory have confirmed that newborn and adult OAEs can be recorded with similar LSF analysis windows and sweep rates (Abdala et al., 2015); as such, the same parameters were used for the two age groups here.

With the goal of reducing the noise floor and eliminating uninformative sources of variability, we processed SFOAEs to focus on the primary reflection at the probe frequency. SFOAE measurements include coherent reflections backscattered from the place on the cochlea associated with the probe frequency (near the peak of the traveling wave) but also longer latency multiple internal reflections (MIRs). MIRs occur when out-going waves reflect from the stapes footplate back into the cochlea; they peak at the probe frequency site and are rereflected basal ward, contributing as a component of the SFOAE measured in the ear canal (Dhar, Talmadge, Long, & Tubis, 2002; Konrad-Martin & Keefe, 2005; Sisto, Sanjust, & Moleti, 2013). MIRs can contaminate estimates of SFOAE delay and the fine structure they produce on the SFOAE spectra is noninformative. In addition to long-latency MIRs, early components of the SFOAE can be contaminated by the probe and suppressor, which overlap in time. To focus on the main reflection site, various signal processing methods have been implemented (e.g., Abdala, Gu rit, Luo, & Shera, 2014; Konrad-Martin & Keefe, 2005; Mishra & Biswal, 2016; Schairer, Ellison, Fitzpatrick, & Keefe, 2006; Shera & Bergevin, 2012). We applied the inverse fast Fourier transform (FFT) to extract the SFOAE and eliminate these artifacts as described below.

SFOAE spectral data were resampled with 10-Hz frequency resolution and overlapping Hann-windowed segments of the response were transformed into the time domain for windowing. The time-domain windows were centered at times given by published SFOAE delay curves (Shera, Guinan, & Oxenham, 2002),  $\tau(f)$ , and varied with frequency according to a power-law function. The time windows used to extract the principal SFOAE spanned the region between the curves  $\tau_{\text{short}} = 0.5\tau(f)$  on the short-latency side and  $\tau_{\text{long}} = 1.5\tau(f)$  on the long-latency side, consistent with the work of Moleti, Longo, and Sisto (2012). The windowed data were then transformed back into the frequency domain using an FFT. The SFOAE noise was passed through the same time-domain filter as the emissions and served as a reference for SNR measures.

### Data Analysis

SFOAE morphology or ‘‘macrostructure’’ was analyzed with a basic peak-picking algorithm. We identified

spectral peaks (having 6 dB SNR or greater) that extended at least 2 dB from the minimum or valley on either side to calculate the number of SFOAE peaks per octave. The referent noise floor was calculated as the median of a 100 Hz noise band centered on the peak frequency. The fractional frequency spacing between peaks was also assessed and calculated as the geometric mean frequency of two sequential peaks,  $\text{Peak}_1$  and  $\text{Peak}_2$  ( $f$ ), divided by the frequency difference ( $\Delta f$ ) between them ( $f/\Delta f$ ); larger values indicate narrower spacing. A loess trend line was fit to the individual spacing values to guide the eye and elucidate trends.

We calculated SFOAE level both as full spectra (with  $\sim 400$  data points) and binned into third-octave frequency bands. The binned frequency bands allowed for statistical analysis with a two-way Age  $\times$  Frequency analysis of variance (ANOVA). SFOAE phase (cycles) was plotted as a function of frequency for all subjects and two indices were calculated: (a) phase accumulation in cycles and (b) phase slope in cycles/kHz. Both measures were tested for age effects with a one-way ANOVA. SFOAE phase was converted to group delay by calculating the negative of the slope of the phase as  $\tau(f) = -d\phi_{\text{SFOAE}}(f)/df$ , where  $\phi_{\text{SFOAE}}(f)$  is SFOAE phase in cycles. Following the convention of Shera and Guinan (2003), SFOAE delays were then expressed in dimensionless form as the equivalent number of periods of the stimulus frequency:  $N_{\text{SFOAE}}(f) = f \cdot \tau(f)$ . The normalized delays were described by fitting trend lines to data points at peaks in the amplitude spectra only (those with at least 6 dB SNR); this strategy has shown to effectively reveal the underlying trend in SFOAE delay across frequency (Shera & Bergevin, 2012).

Finally, to identify the apical–basal transition frequency from the SFOAE delay data, the normalized SFOAE delay was fit with two intersecting power laws (i.e., two straight lines on log–log axes). The point of intersection between lines was a free parameter and represents the frequency at which the slope of the SFOAE delay changes. The intersection frequency estimates the putative apical–basal ( $a|b$ ) transition. The high-frequency segment is thought to be approximately scaling symmetric, whereas the segment below the  $a|b$  transition or “seam” deviates from scaling behavior (Abdala, Dhar, & Mishra, 2011; Shera & Guinan, 2003).

## Results

### Data Cleaning

SFOAE level measures were cleaned by the following method: Each OAE spectrum was composed of roughly 400 points across frequency; single points were eliminated if they failed to meet a 6 dB SNR criteria at the corresponding frequency. This led to 16% of the points

eliminated per neonatal ear (considering only newborns with present SFOAEs). After this initial point-by-point cleaning routine, all remaining data were binned into third-octave frequency bands with 10 center frequencies: 1 kHz, 1.3 kHz, 1.6 kHz, 2 kHz, 2.5 kHz, 3.1 kHz, 4 kHz, 5 kHz, 6.3 kHz, and 8 kHz. If, in any given ear, a third-octave frequency band was comprised of less than half of the original number of data points, this frequency condition was eliminated for that subject. Once the cleaned data were entered into a group database, outliers were identified as values falling  $\pm 2$  SDs from the mean and eliminated: Only three such values were removed.

### SFOAE Prevalence

To estimate the prevalence of SFOAEs in newborns, we separated ears with measurable SFOAEs (sometimes referred to as “present” OAEs) from those with nonmeasurable (i.e., “absent”) SFOAEs. Newborns with SFOAEs in fewer than 5 of the 10 center-frequency conditions were considered to have a nonmeasurable or absent response and those with SFOAEs in at least 5 of the center-frequency conditions had present SFOAEs. Using this somewhat arbitrary distinction, SFOAE prevalence in newborns (at 40 dB SPL) was 83% (24 of 29 ears); 100% of adult subjects had measurable SFOAEs by these same criteria. The median SFOAE SNR for the group of newborns with present SFOAEs ranged from 14 dB (at the highest center frequency, 8 kHz) to 27 dB (at 1.6 kHz; see Figure 1).

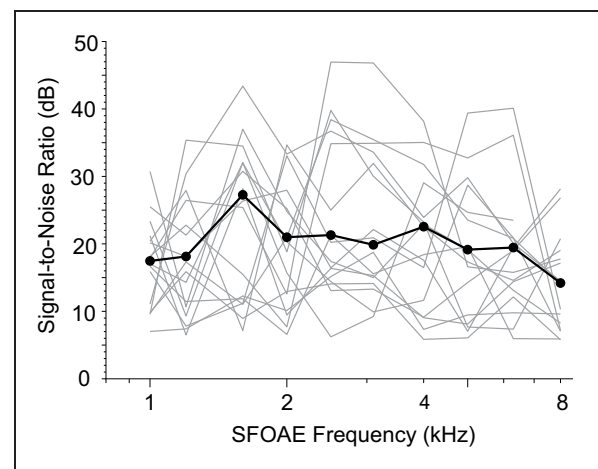


**Figure 1.** Black lines and filled circles display the median neonatal stimulus-frequency otoacoustic emission (SFOAE) signal-to-noise ratios (SNRs) across third-octave frequency bands. The probe level was 40 dB SPL. Only level values at least 6 dB above the noise were used in the calculation of the median. The thin lines in gray are the individual SNRs for the 22 neonatal subjects with measurable SFOAEs.

Two of the 24 newborns with present SFOAEs exhibited excessively high noise floors and developed significant shifts in their probe position during testing; hence, the newborn subject pool was pared down to 22 subjects. Of these 22, 20 had present DPOAEs ( $>6$  dB SNR) for 4/6 test frequencies. In the group with SFOAEs deemed unmeasurable, 5 of the 7 ears failed this DPOAE screen. The DPOAE proved to be a rough predictor of whether SFOAEs would be measurable in a newborn. It is probable that it served as a crude indicator of a clear ear canal and middle ear as well as an index of whether the probe fit and orientation were adequate.

### Probe-Fit Leakage

Experienced neonatal testers found it difficult to achieve a good probe fit and probe stability in neonatal ears with the ER-10X probe assembly. The availability of only one size of probe tip (4 mm diameter, Sanibel red silicone) exacerbated these difficulties because this tip was generally too large to accommodate most newborn ears easily; for this reason, we fashioned a second probe tip with a smaller diameter (3 mm diameter, Sanibel yellow silicone) to fit the ER-10X probe. In general, the long, conical shape, and substantial bulk of the probe head itself was difficult to position in the small, flaccid newborn ear canal and it came unseated easily during testing.

Figure 2(a) shows a stimulus calibration function measured in one neonatal subject. The dashed line is associated with a “leaky” fit and the solid line is characteristic of a snug fit and good seal. A good seal shows relatively flat levels below 2 kHz. The leaky fit shows a downward sloping function below approximately 1.5 kHz, suggestive of reduced low-frequency energy recorded at the microphone. OAE pressure levels sometimes dissipated due to a partially open canal, primarily in the low-frequency range. Groon, Rasetshwane, Kopun, Gorga, and Neely (2015) have confirmed that probe leaks produce an increase in low-frequency absorbance and in the frequency of the air-leak resonance in adult ears. The degree of the effect depends on the size of the leak. Others have found that probe leaks are likely responsible for the largest portion of variance in absorbance measures (Voss, Stenfelt, Neely, & Rosowski, 2013); however, neither of these studies were conducted with infants, which have nonadult-like dimensions and transmission characteristics (see Abdala & Keefe, 2012). There is no doubt that probe leaks are detrimental to the reliable measurement of OAEs in either age-group.

To define the association between probe leakage and SFOAE presence in newborns, Figure 2(b) shows calibration functions separately for the group of 22 infants with present SFOAEs (solid lines) and the seven newborns who were determined to have absent SFOAEs (dashed lines). The thick line displays the mean, while

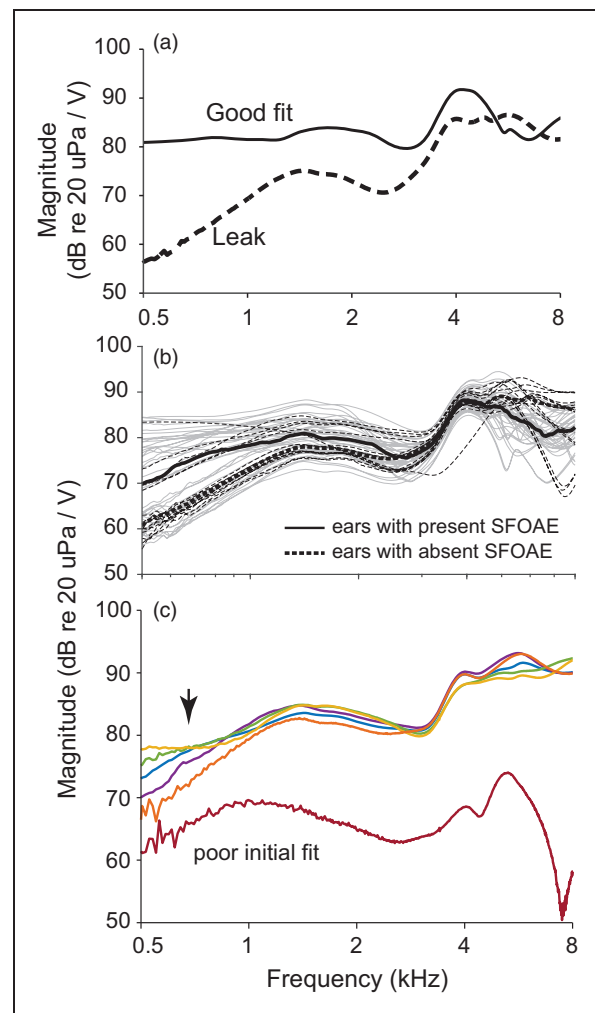


**Figure 2.** (a) The calibration function recorded in the ear canal at the beginning of each test (and intermittently throughout testing) displays the magnitude of the calibration chirp across frequency. The black solid line illustrates a snug, well-coupled fit, which is generally flat below 2 kHz; the dashed illustrates a poor probe fit with leakage of energy in the low frequencies. (b) The mean and individual calibration functions from newborns with measurable stimulus-frequency otoacoustic emissions (SFOAEs): and those with nonmeasurable or absent SFOAEs (The means are shown as the thick solid and dashed lines; and the individual functions as the thin gray and dashed lines.). The central trend is that the group mean for those with nonmeasurable SFOAEs shows leaking, consistent with a poorer seal; and the group mean for newborns with measurable SFOAEs is flatter with less leakage evident. (c) An example of multiple calibration functions measured during data collection in one newborn ear. The initial fit is poor (red) but after a refit (yellow), it improves and the test begins; during the course of testing, due to subject movement and shifts in the probe fit, a leak again develops (see arrow; purple, orange lines).

the thin lines are individual ear functions. The central tendencies are clear: The group eliminated from analysis for not having SFOAEs with sufficient SNR across frequency showed more probe leakage compared with fits

observed in the group with present SFOAEs. This trend is consistent with the idea that leaks in the seal between the probe and the neonatal ear canal generally contribute to a poor OAE outcome.

Because an SFOAE recording did not commence until the probe fit was deemed adequate (as per multiple screening indices), the initial fit was good; however, because this probe did not seat particularly well in infant ears, its position sometimes shifted during testing. Figure 2(c) shows a typical series of calibration functions recorded in one neonatal ear during data collection. The initial fit is poor (red) but gets better after refitting (orange and yellow) and appears leak free for part of the test. During data collection, a shift in the fit occurred, initiating leakage once again (green, blue, and purple). In many ears, the probe was repeatedly refit.

### Ear Canal Reflectance

We used pressure reflectance values recorded with each probe fit to calculate ear-canal energy reflectance, which is the square of the pressure reflection coefficient (Keefe, Bulen, Arehart, & Burns, 1993). Energy reflectance can provide an indicator of probe orientation (i.e., wedged against or near the ear canal), pressure changes in the ear canal, or the presence of ear canal/middle-ear debris and fluid (Aithal, Aithal, Kei, & Manuel, 2019; Hunter, Keefe, Feeney, & Fitzpatrick, 2017; Myers et al., 2019b; Sanford & Feeney, 2008) and has been reliably associated with poor OAE outcomes (Keefe & Simmons, 2003; Myers et al., 2019a). Figure 3 shows the mean magnitude of the energy reflectance for the newborn group with present SFOAEs (solid black) and those with absent SFOAEs (dashed). Newborns are expected to have relatively low and flat reflectance values across frequency compared with adults due to immaturities in both ear-canal and middle-ear vibration (Keefe & Abdala, 2007; Keefe et al., 1993). However, the group of newborns with unmeasurable SFOAEs had higher reflectance overall relative to their peers with present SFOAEs. This result may indicate a poorer fit or debris in the conductive pathway for this subset of subjects because reflectance is expected to be higher when the probe is oriented up against the ear canal or when fluid/debris is present (Wang, Keefe, & Gan, 2016).

### SFOAE Macrostructure

Figure 4(a) and (b) displays examples of SFOAE spectra from an adult (top panel) and three newborns with strong, fair, and poor SFOAEs. The strong newborn SFOAE in Panel b is robust with adequate SNR across much of the frequency range; a more typical SFOAE result is shown in Panel c. It has adequate SNR across a more restricted range. A poor SFOAE is

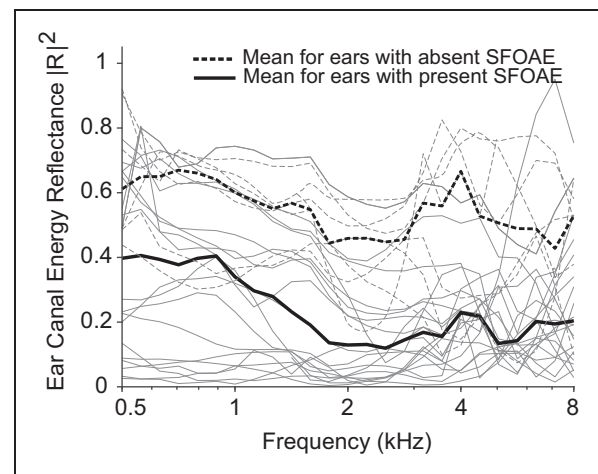
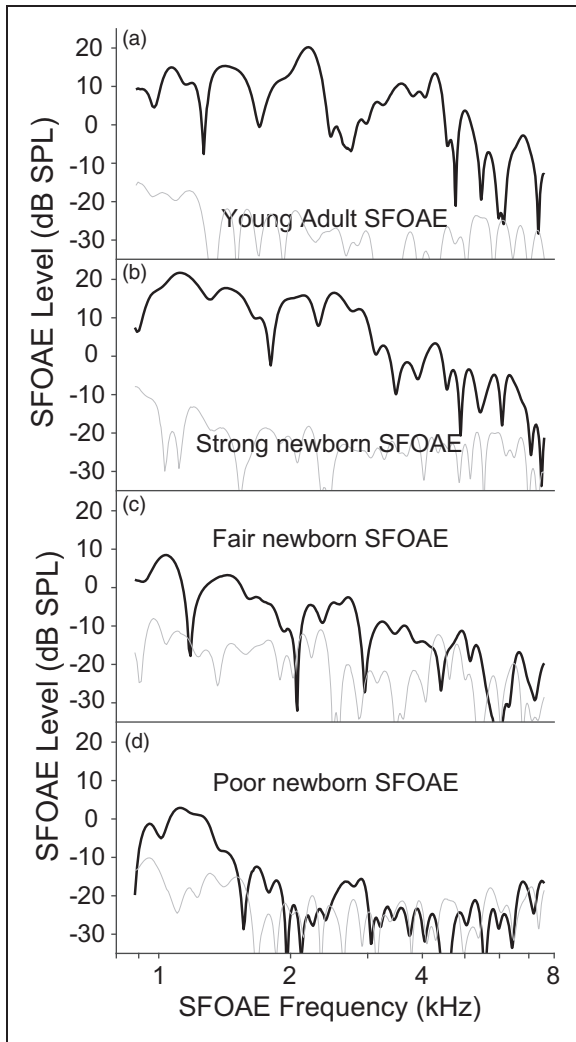


**Figure 3.** Mean (thick lines) and individual (thin lines) wideband energy reflectance measured in the ear canal of newborns with measurable (solid lines) and nonmeasurable (dashed lines) stimulus-frequency otoacoustic emissions (SFOAEs). Ear canal energy reflectance is higher overall in the group with inadequate SNR across the frequency range. Higher reflectance may suggest debris/fluid in the ear canal or a poorly oriented fit (i.e., wedged against the ear-canal wall).

shown in Panel d where emissions have sufficient SNR over less than half of the spectral range. To quantify the morphology of the SFOAE, we calculated the distribution of SFOAE peaks across frequency and their spacing in the newborn and adult groups (Figure 5). (Note that all SFOAE features characterized in newborns include only the 22 subjects with measurable SFOAEs as per our established definition.) Figure 5(a) shows a histogram of the percentage of SFOAE peaks (out of the total number) per octave. For both age groups, the number of peaks increases as frequency increases. The largest proportion of peaks (nearly 40% of them) falls in the highest octave from 4 to 8 kHz for both newborns and adults. Figure 5(b) shows the fractional spacing between SFOAE peaks. For both adults and newborns, spacing between SFOAE peaks decreases with increasing frequency. Between 1 and 7 kHz, the median value of  $f/\Delta f$  doubles indicating systematically narrower spacing as frequency increases. This result is consistent with a greater number of peaks per octave at high frequencies. The spacing of SFOAE peaks is not greatly different between adults and infants except at the highest frequencies, where the trend shows slightly narrower spacing for newborns. In general, the morphology of the newborn SFOAE is comparable to that of the adult's.

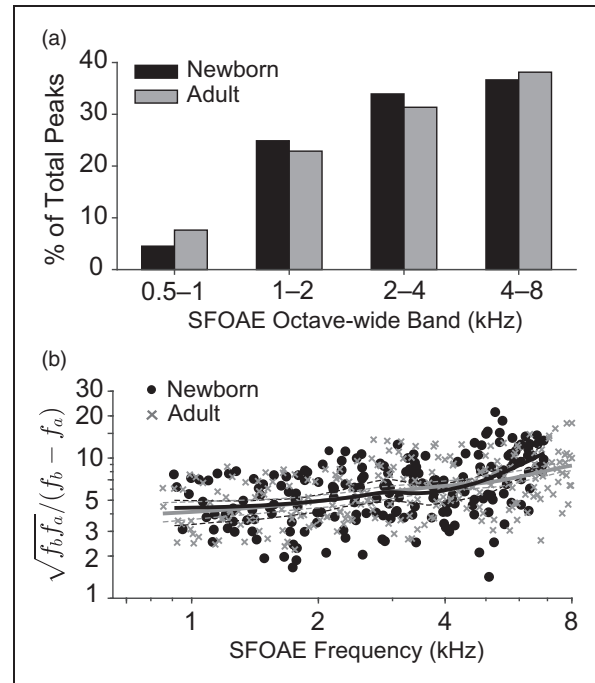
### SFOAE Level

Figure 6 displays individual SFOAE amplitude spectra (for a 40 dB SPL probe) from newborn subjects; a loess



**Figure 4.** Stimulus-frequency otoacoustic emission (SFOAE) spectra for (a) one adult and (b to d) three newborns. For both age groups, the strongest SFOAE amplitudes were almost always in the low to mid frequencies with a decline above approximately 4 to 6 kHz. The infant in Panel b shows a strong SFOAE (higher in level than the adult shown in Panel a) whereas infants in Panels c and d provide exemplars with fair and poor SFOAEs, respectively.

line has been fit to these data to visualize the trend (see thick black line). A gray loess line is also displayed for adult data though individual adult data are not shown. The 95% confidence intervals (dashed lines) were generated through resampling of the data. Both age groups show the strongest SFOAEs between 1 and 2 kHz, consistent with past work (Abdala, Guardia, et al., 2018; Dewey & Dhar, 2017; Ellison & Keefe, 2005). Between 3 and 5 kHz, adults show higher levels than newborns, likely due to standing-wave interference in the ear canals of these adult subjects. The interference between forward-going stimulus waves and those reflected from the tympanic membrane produces miscalculations in



**Figure 5.** (a) Histogram showing the number of stimulus-frequency otoacoustic emission (SFOAE) peaks as a percentage of total peaks present in four frequency-bands in the newborn (black) and adult (gray) groups. The number of peaks increases as frequency increases for both age groups. (b) The fractional spacing between SFOAE peaks is shown for both age groups; the larger the value, the narrower the spacing. Loess trend lines have been fit to newborn (black) and adult (gray) individual data to visualize trends (dashed lines are 95% confidence intervals). In general, SFOAE peak spacing for adults and newborns is similar at all but the highest frequencies where newborns diverge and show slightly narrower spacing.

stimulus level, in particular for stimuli around the quarter wave null near 3 to 4 kHz in adults (Scheperle, Neely, Kopun, & Gorga, 2008). Forward-pressure-level calibration can correct for standing-wave interference, and we have used this method routinely in our laboratory for adult data collection (Maxim, Shera, Charaziak, & Abdala, 2019); however, standing-wave interference does not occur in the shorter newborn ear canal at the same frequencies. Because the neonatal ear canal is approximately 1.7 cm long, which is only two thirds of the adult length (Crelin, 1973), standing-wave interference (and its pernicious influence on estimates of stimulus level) will occur only for frequencies  $>6$  kHz in newborns (Siegel, 1994); therefore, they will not get this same effective “boost” in SFOAE amplitude at 3 to 4 kHz. The forward-pressure-level calibration method has not been tested in newborn ears to assess its effectiveness. For this reason, here we calibrated stimulus level in both age groups using a conventional SPL measure taken at the microphone but consider the effects

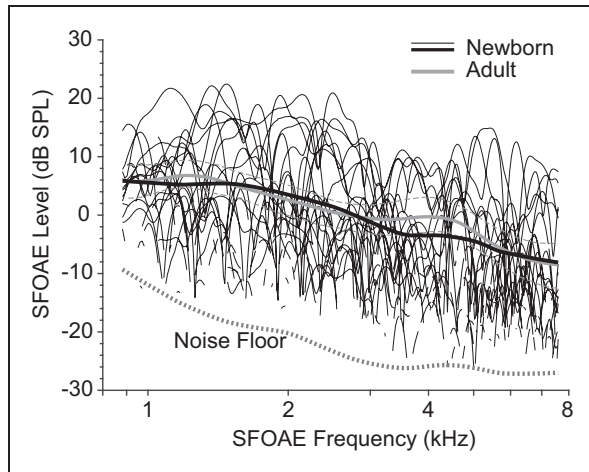


**Figure 6.** Individual stimulus-frequency otoacoustic emission (SFOAE) spectra (thin lines) generated with a probe at 40 dB SPL for all newborn subjects with present SFOAEs. A loess trend line is fit to the neonatal SFOAE level values and a fit to adult data is also provided though individual adult spectra are not shown. Dashed lines indicate 95% confidence intervals. Overall, newborn and adult SFOAE levels appear to overlap across frequency.

of standing-wave interference on our age comparisons. This interference results in a higher than-intended stimulus level presented to the adult cochlea (Charaziak & Shera, 2017), which probably contributes to the slightly higher adult SFOAE levels around 4 kHz.

Figure 7 shows SFOAE level segmented into third-octave frequency bands for analysis. The figure also includes an alternative calculation of SFOAE level at peaks in the spectra only (open circles). Mean amplitude values from Kalluri and Abdala (2015), who measured discrete-tone SFOAEs in one narrow frequency range at spectral peaks only, are also included. As expected, peak-only SFOAE measures are higher in level by several dB compared with the binned data including amplitude estimates at both peaks and valleys in SFOAE macrostructure. Adult SFOAE levels from Kalluri and Abdala (black “x”) match well with that of our adult subjects within the narrow range of common frequencies; however, newborn SFOAEs tested in this study (inverted triangles) are reduced in amplitude compared with neonatal data collected in the earlier study.

A two-way Age (2)  $\times$  Frequency (10) ANOVA was conducted on SFOAE levels in third-octave frequency bands and found no significant difference between adult and newborn SFOAE levels ( $f=3.69$ ;  $p=.06$ ) and no interaction between frequency and age. The near significance of the age effect can probably be accounted for by the greater adult SFOAE levels between 3 and 4 kHz (which we attribute to ear canal acoustics rather than cochlear function). Overall, the analysis suggests that newborn SFOAE amplitudes are basically adult-like,

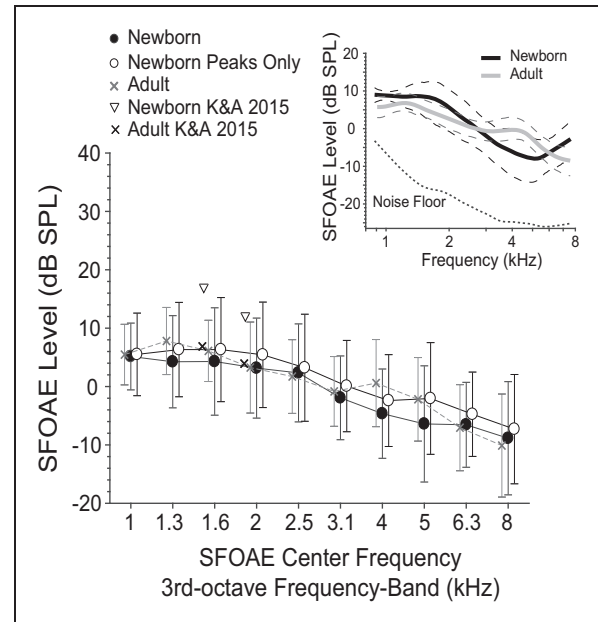


**Figure 7.** The main figure shows stimulus-frequency otoacoustic emission (SFOAE) level ( $\pm 1$  SD) binned into third-octave frequency bands for newborns (black filled circles) and adults (gray X, dashed lines). The open circles show SFOAE amplitude when it is calculated at only peaks in the SFOAE spectra (vs. third-octave binning that includes peaks and valleys). The inverted triangles and black “X” are SFOAE mean data for newborns and adults from Kalluri and Abdala (2015), which measured SFOAEs evoked with discrete tones over a narrow frequency range. The inset panel shows a loess trend line fit to adults (gray) and a subset of nine newborns (black) with the best probe fittings (and no evident leak). Dashed lines provide 95% confidence intervals. SFOAE levels in this subset of newborns are generally higher than that of adults by 3 to 4 dB except in the 3 to 5 kHz frequency range (note “hump” in gray line). This hump is due to inaccuracies of stimulus level produced by ear-canal standing-wave interference in adult subjects.

which is in contrast to previous work reporting higher level SFOAEs in newborns (Kalluri & Abdala, 2015). The inset of Figure 8 offers one explanation. The inset shows an adult–newborn SFOAE level comparison including data from only the nine infants with the most stable probe coupling to the ear canal (determined based on the calibration functions and tester notes). This analysis shows newborn SFOAE levels that are 3 to 4 dB higher than adult levels at all frequencies (except those impacted by the standing-wave interference).

SFOAEs evoked by a 20 dB SPL probe were also measured in seven newborns (a subset of the neonatal pool of 22 ears). The mean levels across these seven subjects ranged from  $-3$  dB at 1 kHz to  $-15$  dB at 4 kHz. Even though SFOAE levels were low at this stimulus level, SNR was often adequate for reliable measurement. SFOAEs evoked with 20 dB SPL were present in at least

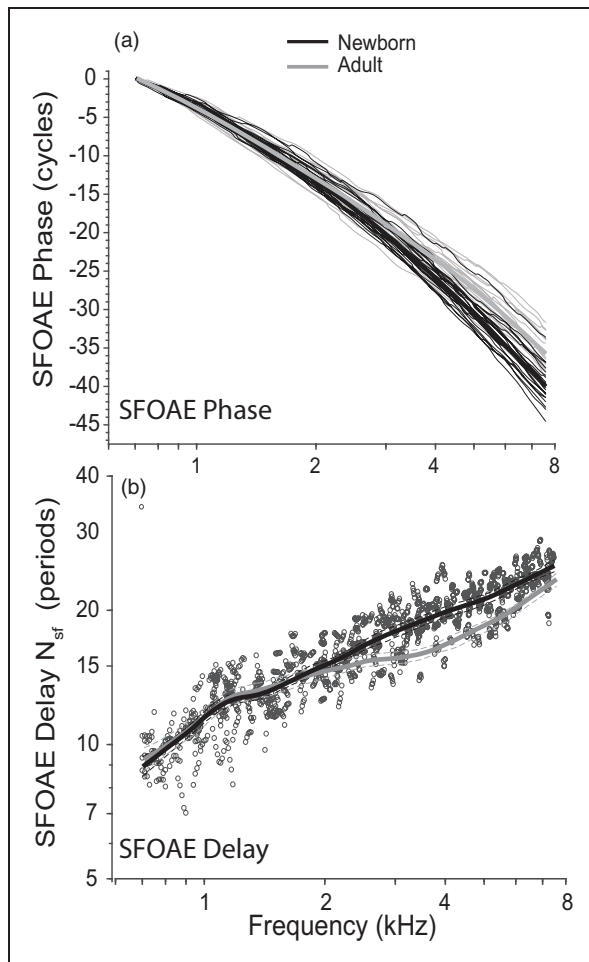


**Figure 8.** (a) Stimulus-frequency otoacoustic emission (SFOAE) phase as a function of frequency for all newborns and adults (thin black and gray lines respectively) with a loess line fit separately to the data from each age-group (thick lines). The mean phase accumulation for the newborn group over the same range of frequencies was significantly greater by approximately three to four cycles. (b) Individual SFOAE delay values normalized by frequency are shown for newborns (circles) but not adults at 40 dB SPL. Loess trend lines were calculated at SFOAE spectral peaks only and are fit to the delay data for both age groups. SFOAE delays below approximately 2 kHz are comparable between age groups, while above 2 kHz newborn SFOAEs show longer delays than adults by two to three periods.

half of the 10 center-frequency conditions for four of the seven newborns tested. Center frequencies such as 1.6 kHz, where SFOAEs are at their peak amplitude, included data with adequate SNR for all seven subjects. As expected, the highest frequency conditions (5, 6.3, and 8 kHz) had the lowest number of ears meeting criterion SNR.

### SFOAE Phase and Delay

Figure 8(a) displays SFOAE phase as a function of frequency in newborn and adult subjects. The starting

phase was set to  $0 \pm 0.5$  cycles at 0.7 kHz. The mean accumulation of phase between 0.7 and 7.6 kHz was 40 cycles ( $SD = 1.99$ ) in newborns compared with only 35.9 cycles ( $SD = 2.3$ ) in adults. Both a phase accumulation index and the slope of the phase were calculated across frequency and tested for age effects. We found a significant age effect on phase accumulation ( $F = 28.8$ ;  $p < .001$ ) and slope of phase (cycles/kHz:  $F = 51$ ;  $p < .001$ ) both, confirming that newborns have a significantly steeper SFOAE phase gradients and longer delays than adults.

SFOAE delay was calculated and expressed as a dimensionless variable measured in periods of the stimulus frequency (Shera & Guinan, 2003; see “Methods” section). [The normalization process is equivalent to computing the phase slope on a log-frequency axis:  $N_{SF} = -d\phi_{SFOAE}/d\ln f$ .] Figure 8(b) displays the individual values of the normalized SFOAE delay,  $N_{SF}$ , in the neonatal group (for a 40 dB SPL probe); loess trend lines are superimposed on the group data to elucidate the underlying delay trends. For the low frequencies, the delays are comparable between age groups and range from approximately 9 to 15 cycles. For frequencies  $> 2$  kHz, however, newborns show longer delays than adults by two to three periods.

### The Apical-Basal Seam

Past work has identified a “bend” in the trajectory of normalized SFOAE delays across frequency in adults, roughly near the midpoint of the cochlea ( $\sim 1$  kHz; Abdala, Guardia, et al., 2018; Shera & Guinan, 2003). A similar discontinuity in the phase of the DPOAE across frequency has also been observed (Abdala et al., 2011; Christensen, Abdala, & Shera, 2018; Dhar, Rogers, & Abdala, 2011). The frequency at which this bend in phase/delay is noted is thought to represent an apical–basal transition in the mammalian cochlea. The basal half of the cochlea shows approximate scaling, whereas the apical half does not. Local scaling symmetry at its most basic indicates that any tone will accumulate the same number of cycles irrespective of its frequency (Zweig, 1976), that is, traveling wave patterns no matter where they peak on the basilar membrane are shift similar and share the same shape or form if normalized and superimposed. Below approximately 1 to 2 kHz, scaling symmetry assessed with OAE measures does not hold. Past work has characterized this apical–basal seam in newborns through elderly adults by measuring the phase of the DPOAE distortion component (Abdala & Dhar, 2012). However, the apical–basal seam has not been described in newborns using SFOAE delays. Figure 9 shows the same kind of delay data displayed in Figure 8(b), but the delay values are fit with two straight lines on a log–log axis. The intersection of these

two power-law functions defines the putative apical–basal transition frequency. As noted in Figure 9, estimates of the apical–basal demarcation are comparable in newborns and adults and are centered near 1 kHz.

### Summary of Results

To summarize the results, the prevalence of SFOAEs in newborns was 83% though we believe it would have been higher with stable probe fittings in all 29 infant subjects. The overall morphology of the SFOAE was similar in adults and newborns as was the apical–basal transition frequency. SFOAE levels in newborn ears were slightly higher than adult levels when considering only neonatal subjects with the most firmly coupled and stable probe fits; and SFOAE delays were longer in newborns than adults for stimuli above 2 kHz. We also found associations between the presence of SFOAEs in newborns and both abnormal ear-canal energy reflectance and probe leakage. This association suggests that those neonates lacking measurable SFOAEs may have had debris/fluid in the ear canal/middle ear or an unstable probe fit.

### Discussion

SFOAEs are measurable in the great majority of newborns tested. Although we initially derived a prevalence

estimate of 83%, it is likely that SFOAEs are present in healthy newborns at the same rate as are other reflection emissions, roughly 90% to 100% (e.g., Abdala, Luo, & Shera, 2017; Kemp, 1978; Norton & Neely, 1987). In fact, if we redefine SFOAE presence, our estimate of course changes. Considering the natural decline in SFOAE amplitude at high frequencies, one might choose to include only the seven frequency bands between 1 and 4 kHz to classify SFOAEs and accept adequate SNR in four of these seven frequencies as indication of a “present” response. In this alternative scenario, SFOAE prevalence in newborns is 90%. Hence, we surmise that the lower than expected 83% prevalence initially reported is due to a combination of a difficult-to-fit probe assembly, which is not presently well suited for newborn ears, and our rather arbitrary definition of what constitutes a present or measurable SFOAE. Overall, our results confirm that robust stimulus-frequency OAEs can be recorded in nearly all neonatal ears using rapidly swept tones and that newborn SFOAEs resemble adult SFOAEs in their general morphology.

### Adaptations to SFOAE Measurement in Newborns

An important consideration in measuring SFOAEs in newborns is the technique with which SFOAEs are extracted. The interleaved suppression method involves four sequential intervals:  $p_1$  = probe tone alone,  $p_2$  = probe and suppressor tone (+polarity),  $p_3$  = probe tone alone, and  $p_4$  = probe and suppressor tone (–polarity). The SFOAE time waveform is extracted using the formula:  $p_{\text{SFOAE}} = (p_1 + p_3 - p_2 - p_4)/2$ . To work effectively, this method assumes that the probe and suppressor (as well as the SFOAE generated by the cochlea) are the same with respect to phase and amplitude in each of the four intervals, which is not unreasonable for a cooperative adult. If baby movement and consequent probe shifts occur during this sequence of four, which is 4.5 s long in our protocol, the extraction of the SFOAE (which requires canceling the probe tone), can be incomplete and the calculated residual in error. In these cases, the measured “SFOAE” can include a strong artifact from the probe tone.

Several steps can be taken to mitigate the effects of this potential contaminant. First, it will be critical in successfully recording SFOAEs in newborns to minimize the time between probe and suppressor intervals so as to extract the SFOAE completely and reduce the impact of probe shifts during the recording interval. Second, it will be important to use postprocessing of the SFOAE to eliminate probe tone artifacts if they do contaminate a recording. Using rapidly sweeping tones as stimuli can optimally satisfy the first condition. The second condition can be achieved by signal processing such as the inverse FFT we used in this study. The time-domain

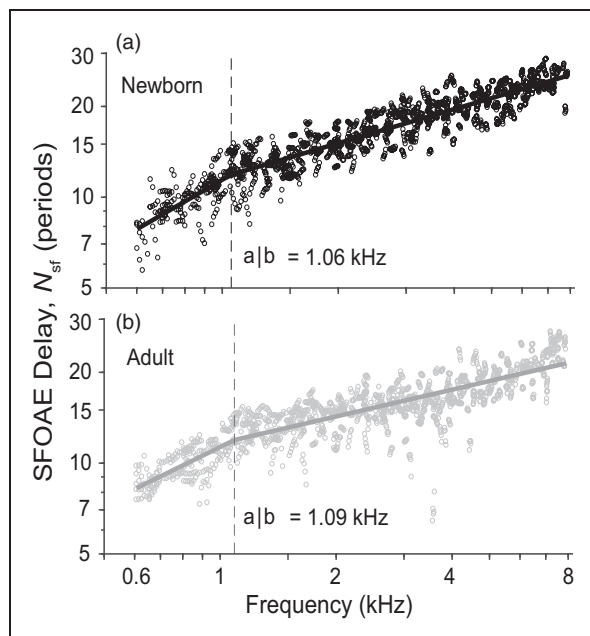


**Figure 9.** Individual normalized stimulus-frequency otoacoustic emission (SFOAE) delay values for (a) newborns and (b) adults fit by two straight lines on a log–log axis. (Note that only SFOAE data with at least 6 dB SNR contributed to this analysis.) The point of intersection between lines represents the frequency at which the slope of the SFOAE delay changes; it provides an estimate of the putative apical–basal ( $a|b$ ) transition frequency.

filters on the short-latency boundary effectively eliminated probe-related energy that might have contaminated the SFOAE. This is evidenced by the long SFOAE delays measured in newborn and adult subjects. A third adaptation is frequent recalibration during data collection with newborns to recalculate the voltage required to reach target levels as probe shift occurs. Probe movement is inevitable and frequent calibration can accommodate these shifts. A fourth necessary step to adapt SFOAE measurement to newborns is an effective artifact-rejection strategy to further protect against spurious noise and artifacts. In this study, most artifacts contaminating our SFOAE measures, including those that might be probe tone related, were eliminated by our off-line artifact-rejection criteria; recall that any spike extending four *SDs* from the median SFOAE level was eliminated.

### Cochlear Immaturity

The primary tools we have utilized to study functional maturation of the human cochlea over the last two decades have included DPOAEs, which are generated by the compressive nonlinearity of outer hair cells, and the separated reflection component of the DPOAE, which is a reflection-source emission much like the SFOAE. Unmixing the DPOAE to derive the reflection component suffers from many shortcomings as noted in the “Introduction” section. This work used a more direct and less confounded reflection emission, the SFOAE, to examine functional maturation of the human cochlea at birth. Our SFOAE results verify that neonatal reflection emissions are at least as high in level as they are in adults and when optimally measured (with a firm and stable probe tip), they are higher in level by 3 to 4 dB. This suggests that cochlear reflections near the peak of the traveling wave elicited by the SFOAE probe are robust in newborns, which is consistent with strong cochlear gain. One potential confound is ear-canal area or volume, which differs by more than a factor of seven between term newborns and adults (Keefe & Abdala, 2007). The emerging SFOAE encounters a smaller ear-canal cavity in newborns (compared with adults), which effectively boosts emission pressure levels measured at the microphone. Hence, the SFOAEs observed here in newborns partly reflect a boost in level conferred by immaturities of ear-canal size.

According to theory, robust reflections are also consistent with strong cochlear gain and sharp tuning. Linear coherent reflection theory (Shera & Guinan, 1999; Talmadge, Tubis, Long, & Piskorski, 1998) associates the phase slope of the SFOAE with the phase slope of the traveling wave transfer function near the peak of the traveling wave where SFOAEs are thought to arise (Shera & Zweig, 1993). The theory predicts that

delays of the basilar membrane mechanical transfer function are in turn related to tuning: the steeper the slope, the sharper the tuning. This reciprocal relationship also dictates that both measures (group delays and tuning) should respond in a predictable way to stimulus level. SFOAEs have, in fact, shown strong level dependence, becoming more delayed at lower levels (Abdala, Guardia, et al., 2018; Schairer et al., 2006; Sisto & Moleti, 2007).

Neonates in this study showed steeper SFOAE phase slope and longer group delays than adults. This has also been reported in past work examining the separated reflection component of the DPOAE (Abdala & Dhar, 2012), but the unmixing technique can include confounds. Measurement of the less confounded SFOAE confirms that longer delays are unequivocally present for newborns above approximately 2 kHz. This result can be difficult to interpret and is no doubt influenced by immaturities of the conductive pathway detailed earlier; that is, the immature middle ear impacts the forward transmission of the stimulus, presenting the neonatal cochlea with a lower level signal (re: adult levels). Because SFOAE delays are level-dependent, this immaturity results in longer delays (Abdala, Guardia, et al., 2018; Kalluri & Shera, 2007; Schairer et al., 2006; Schairer, Fitzpatrick, & Keefe, 2003).

Although it is clear that the neonatal emissions are shaped to some extent by these conductive immaturities, nonadult-like SFOAE characteristics in newborns likely reflect residual cochlear immaturities as well. A recent study of human neonatal temporal bones described morphological immaturities and postnatal refinement of cochlear architecture around the time of birth (Meenderink, Shera, Valero, Liberman, & Abdala, 2019). Structural immaturities included a slightly wider and thinner basilar membrane in newborns. This immaturity could create a more compliant newborn organ of Corti, which is consistent with the longer OAE delays observed in neonates across multiple studies. It is probable that a combination of subtle morphological immaturities and the shaping imposed by immature conductive pathways account for the immature SFOAE characteristics observed here in neonates: higher SFOAE levels and longer SFOAE delays.

Finally, it is striking (and consistent with past work) that the apical–basal, *a/b*, transition frequency is similar in day-old newborns and adults, as gauged by SFOAE delays (Figure 9). DPOAE phase-frequency functions demarcating this *a/b* transition have also shown consistency throughout the human life span (Abdala & Dhar, 2012).

### Conclusions

This study represents the first comprehensive report of swept-tone SFOAEs in newborns. It is a preliminary step

toward a more comprehensive study assessing the clinical utility of SFOAEs in newborns. Although we showed that swept-tone SFOAEs can be successfully recorded at birth, a large-scale study with normal-hearing and hearing-impaired infants is required to determine their performance in the detection of hearing loss. Here, we characterized prevalence, normative amplitude, phase, and delay in newborns and suggest adaptations to SFOAE protocol for successful measurement in this age-group. Most importantly, we considered how the results inform our understanding of cochlear maturation. Consistent with past work, we found larger amplitude SFOAEs in newborns than adults and longer group delays. We believe these findings reflect conductive immaturities but also late stages of cochlear maturation.

### Acknowledgments

The authors would like to acknowledge support and expertise from University of Southern California + Los Angeles County neonatologist, Dr. Rangasamy Ramanathan, and helpful discussions with Christopher Shera (who also reviewed early drafts of this manuscript) and Karolina Charaziak.

### Declaration of Conflicting Interests

The authors declared no potential conflicts of interest with respect to the research, authorship, and/or publication of this article.

### Funding

The authors disclosed receipt of the following financial support for the research, authorship, and/or publication of this article: This work was supported by the National Institutes of Health (R01 DC003552).

### ORCID iD

Carolina Abdala  <https://orcid.org/0000-0002-1269-8886>

### References

- Abdala, C. (1998). A developmental study of DPOAE (2f1-f2) suppression in humans. *Hearing Research, 121*, 125–138. doi:10.1016/S0378-5955(98)00073-2
- Abdala, C. (2000). Distortion product otoacoustic emission (2f1-f2) amplitude growth in human adults and neonates. *Journal of the Acoustical Society of America, 107*, 446–456. doi:10.1121/1.428315
- Abdala, C., & Dhar, S. (2012). Maturation and aging of the human cochlea: A view through the DPOAE looking glass. *Journal of Association for Research in Otolaryngology, 13*, 403–421. doi:10.1007/s10162-012-0319-2
- Abdala, C., Dhar, S., & Mishra, S. (2011). The breaking of cochlear scaling symmetry in human newborns and adults. *Journal of the Acoustical Society of America, 129*, 3104–3114. doi:10.1121/1.3569737
- Abdala, C., Guardia, Y. C., & Shera, C. A. (2018). Swept-tone stimulus-frequency otoacoustic emissions: Normative data and methodological considerations. *Journal of the Acoustical Society of America, 143*, 181–192. doi:10.1121/1.5020275
- Abdala, C., Guérit, F., Luo, P., & Shera, C. A. (2014). Distortion-product otoacoustic emission reflection-component delays and cochlear tuning: Estimates from across the human lifespan. *Journal of the Acoustical Society of America, 135*, 1950–1958. doi:10.1121/1.4868357
- Abdala, C., & Kalluri, R. (2017). Towards a joint reflection-distortion otoacoustic emission profile: Results in normal and impaired ears. *Journal of the Acoustical Society of America, 142*, 812–824. doi:10.1121/1.4996859
- Abdala, C., & Keefe, D. H. (2006). Effects of middle-ear immaturity on distortion-product otoacoustic emission suppression tuning in infant ears. *Journal of the Acoustical Society of America, 120*, 3832–3842. doi:10.1121/1.2359237
- Abdala, C., & Keefe, D. H. (2012). Morphological and functional ear development. In L. Werner, R. Fay, & A. Popper (Eds.), *Human auditory development. Springer handbook of auditory research (Vol. 42)*, pp. 19–59. New York, NY: Springer. doi:10.1007/978-1-4614-1421-6\_2
- Abdala, C., Keefe, D. H., & Oba, S. (2007). Distortion product otoacoustic emission suppression tuning and acoustic admittance in human infants: Birth through six months. *Journal of the Acoustical Society of America, 121*, 3617–3627. doi:10.1121/1.2734481
- Abdala, C., Luo, P., & Shera, C. A. (2015). Optimizing swept-tone protocols for recording distortion-product otoacoustic emissions in adults and newborns. *Journal of the Acoustical Society of America, 138*, 3785–3799. doi:10.1121/1.4937611
- Abdala, C., Luo, P., & Shera, C. A. (2017). Characterizing spontaneous otoacoustic emissions across the human lifespan. *Journal of the Acoustical Society of America, 140*, 1874–1886. doi:10.1121/1.4977192
- Abdala, C., Ortmann, A. J., & Shera, C. A. (2018). Reflection- and distortion-source otoacoustic emissions: Evidence for increased irregularity in the human cochlea during aging. *Journal of Association for Research in Otolaryngology, 19*, 493–510. doi:10.1007/s10162-018-0680
- Aithal, S., Aithal, V., Kei, J., & Manuel, A. (2019). Effect of negative middle ear pressure and compensated pressure on wideband absorbance and otoacoustic emissions in children. *Journal of Speech, Language, and Hearing Research, 62*, 3516–3530. doi:10.1044/2019\_JSLHR-H-18-0426
- Charaziak, K. K., & Shera, C. A. (2017). Compensating for ear-canal acoustics when measuring otoacoustic emissions. *Journal of the Acoustical Society of America, 141*, 515–531. doi:10.1121/1.4973618
- Christensen, A. T., Abdala, C., & Shera, C. A. (2018). Probing apical-basal differences in the human cochlea using DPOAE phase. In C. Bergevin & S. Puria (Eds.), *To the ear and back again—Advances in auditory biophysics (Vol. 1965)*, p. 090006. Melville, NY: American Institute of Physics. doi:10.1063/1.5038495
- Crelin, E. S. (1973). *Functional anatomy of the newborn*. New Haven, CT: Yale University Press.

- Dewey, J. B., & Dhar, S. (2017). Profiles of stimulus-frequency otoacoustic emissions from 0.5 to 20 kHz in humans. *Journal of Association for Research in Otolaryngology*, *18*, 89–110. doi:10.1007/s10162-016-0588-2
- Dhar, S., Rogers, A., & Abdala, C. (2011). Breaking away: Violation of distortion emission phase-frequency invariance at low frequencies. *Journal of the Acoustical Society of America*, *129*, 3115–3122. doi:10.1121/1.3569732
- Dhar, S., Talmadge, C. L., Long, G. R., & Tubis, A. (2002). Multiple internal reflections in the cochlea and their effect on DPOAE fine structure. *Journal of the Acoustical Society of America*, *112*, 2882–2897. doi:10.1121/1.1516757
- Ellison, J. C., & Keefe, D. H. (2005). Audiometric predictions using stimulus-frequency otoacoustic emissions and middle ear measurements. *Ear and Hearing*, *26*, 487–503. doi:10.1097/01.aud.0000179692.81851.3b
- Gorga, M. P., Neely, S. T., Bergman, B., Beauchaine, K. L., Kaminski, J. R., Peters, J., & Jesteadt, W. (1993a). Otoacoustic emissions from normal-hearing and hearing-impaired subjects: Distortion-product responses. *Journal of the Acoustical Society of America*, *93*, 2050–2060. doi:10.1121/1.406691
- Gorga, M. P., Neely, S. T., Bergman, B. M., Beauchaine, K. L., Kaminski, J. R., Peters, J., . . . Jesteadt, W. (1993b). A comparison of transient-evoked and distortion product otoacoustic emissions in normal-hearing and hearing-impaired subjects. *Journal of the Acoustical Society of America*, *94*, 2639–2648. doi:10.1121/1.407348
- Groon, K. A., Rasetshwane, D. M., Kopun, J. G., Gorga, M. P., & Neely, S. T. (2015). Air-leak effects on ear-canal acoustic absorbance. *Ear and Hearing*, *36*, 155–163. doi:10.1097/AUD.0000000000000077
- Hunter, L. L., Keefe, D. H., Feeney, M. P., & Fitzpatrick, D. F. (2017). Pressurized wideband acoustic stapedial reflex thresholds: Normal development and relationships to auditory function in infants. *Journal of Association for Research in Otolaryngology*, *18*, 49–63. doi:10.1007/s10162-016-0595-3
- Kalluri, R., & Abdala, C. (2015). Stimulus frequency OAEs in human newborns. *Journal of the Acoustical Society of America*, *137*, EL78–EL84. doi:10.1121/1.4903915
- Kalluri, R., & Shera, C. A. (2007). Comparing stimulus-frequency otoacoustic emissions measured by compression, suppression, and spectral smoothing. *Journal of the Acoustical Society of America*, *122*, 3562–3575. doi:10.1121/1.2793604
- Kalluri, R., & Shera, C. A. (2013). Measuring stimulus-frequency otoacoustic emissions using swept-tones. *Journal of the Acoustical Society of America*, *134*, 356–368. doi:10.1121/1.4807505
- Keefe, D. H., & Abdala, C. (2007). Theory of forward and reverse middle-ear transmission applied to otoacoustic emissions in infant and adult ears. *Journal of the Acoustical Society of America*, *121*, 978–993. doi:10.1121/1.2427128
- Keefe, D. H., Bulen, J. C., Arehart, K. H., & Burns, E. M. (1993). Ear-canal impedance and reflectance coefficient in human infants and adults. *Journal of the Acoustical Society of America*, *94*, 2617–2638. doi:10.1121/1.407347
- Keefe, D. H., & Simmons, J. L. (2003). Energy transmittance predicts conductive hearing loss in older children and adults. *Journal of the Acoustical Society of America*, *114*, 3217–3238. doi:10.1121/1.1625931
- Kemp, D. T. (1978). Stimulated acoustic emissions from within the human auditory system. *Journal of the Acoustical Society of America*, *64*, 1386–1391. doi:10.1121/1.382104
- Konrad-Martin, D., & Keefe, D. H. (2005). Transient-evoked stimulus-frequency and distortion-product otoacoustic emissions in normal and impaired ears. *Journal of the Acoustical Society of America*, *117*, 3799–3815. doi:10.1121/1.1904403
- Lapsley Miller, J. A., Marshall, L., & Heller, L. M. (2004). A longitudinal study of changes in evoked otoacoustic emissions and pure-tone thresholds as measured in a hearing conservation program. *International Journal of Audiology*, *43*, 307–322. doi:10.1080/14992020400050040
- Lapsley Miller, J. A., Marshall, L., Heller, L. M., & Hughes, L. M. (2006). Low-level otoacoustic emissions may predict susceptibility to noise-induced hearing loss. *Journal of the Acoustical Society of America*, *120*, 280–296. doi:10.1121/1.2204437
- Long, G. R., Talmadge, C. L., & Lee, J. (2008). Measuring distortion product otoacoustic emissions using continuously sweeping primaries. *Journal of the Acoustical Society of America*, *124*, 1613–1626. doi:10.1121/1.2949505
- Maxim, T., Shera, C. A., Charaziak, K. K., & Abdala, C. (2019). Effects of forward-and emitted-pressure calibrations on the variability of otoacoustic emission measurements across repeated probe fits. *Ear and Hearing*, *40*, 1345–1358. doi:10.1097/AUD.0000000000000714
- Meenderink, S., Shera, C. A., Valero, D. M., Liberman, M. C., & Abdala, C. (2019). Morphological immaturity of the neonatal organ of Corti and associated structures in humans. *Journal of Association for Research in Otolaryngology*, *20*, 461–474. doi:10.1007/s10162-019-00734-2
- Mishra, S. K., & Biswal, M. (2016). Time-frequency decomposition of click evoked otoacoustic emissions in children. *Hearing Research*, *335*, 161–178. doi:10.1016/j.heares.2016.03.003
- Mishra, S. K., & Talmadge, C. L. (2018). Sweep-tone evoked stimulus frequency otoacoustic emissions in humans: Development of a noise-rejection algorithm and normative features. *Hearing Research*, *338*, 42–49. doi:10.1016/j.heares.2017.11.006
- Moleti, A., Longo, F., & Sisto, R. (2012). Time-frequency domain filtering of evoked otoacoustic emissions. *Journal of the Acoustical Society of America*, *132*, 2455–2467. doi:10.1121/1.4751537
- Myers, J., Kei, J., Aithal, S., Aithal, V., Driscoll, C., Khan, A., . . . Malicka, A. N. (2019a). Diagnosing conductive dysfunction in Infants using wideband acoustic immittance: Validation and development of predictive models. *Journal of Speech, Language, and Hearing Research*, *62*, 3607–3619. doi:10.1044/2019\_JSLHR-H-19-0084
- Myers, J., Kei, J., Aithal, S., Aithal, V., Driscoll, C., Khan, A., . . . Malicka, A. N. (2019b). Longitudinal development of wideband absorbance and admittance through infancy.

- Journal of Speech, Language, and Hearing Research*, 62, 2535–2552. doi:10.1044/2019\_JSLHR-H-18-0480
- Norton, S. J., & Neely, S. T. (1987). Tone-burst-evoked otoacoustic emissions from normal-hearing subjects. *Journal of the Acoustical Society of America*, 81, 1860–1872. doi:10.1121/1.394750
- Sanford, C. A., & Feeney, M. P. (2008). Effects of maturation on tympanometric wideband acoustic transfer functions in human infants. *Journal of the Acoustical Society of America*, 124, 2106–2122. doi:10.1121/1.2967864
- Schairer, K. S., Ellison, J. C., Fitzpatrick, D., & Keefe, D. H. (2006). Use of stimulus-frequency otoacoustic emission latency and level to investigate cochlear mechanics in human ears. *Journal of the Acoustical Society of America*, 120, 901–914. doi:10.1121/1.2214147
- Schairer, K. S., Fitzpatrick, D. H., & Keefe, D. H. (2003). Input-output functions for stimulus-frequency otoacoustic emissions in normal-hearing adult ears. *Journal of the Acoustical Society of America*, 114, 944–966. doi:10.1121/1.1592799
- Scheperle, R. A., Neely, S. T., Kopun, J. G., & Gorga, M. P. (2008). Influence of in situ, sound-level calibration on distortion-product otoacoustic emission variability. *Journal of the Acoustical Society of America*, 124, 288–300. doi:10.1121/1.2931953
- Shera, C. A., & Bergevin, C. (2012). Obtaining reliable phase-gradient delays from otoacoustic emissions data. *Journal of the Acoustical Society of America*, 132, 927–943. doi:10.1121/1.4730916
- Shera, C. A., & Guinan, J. J. (1999). Evoked otoacoustic emissions arise by two fundamentally different mechanisms: A taxonomy for mammalian OAEs. *Journal of the Acoustical Society of America*, 105, 782–798. doi:10.1121/1.426948
- Shera, C. A., & Guinan, J. J. (2003). Stimulus-frequency-emission group delay: A test of coherent reflection filtering and a window on cochlear tuning. *Journal of the Acoustical Society of America*, 113, 2762–2772. doi:10.1121/1.1557211
- Shera, C. A., Guinan, J. J., & Oxenham, A. J. (2002). Revised estimates of human cochlear tuning from otoacoustic and behavioral measurements. *Proceedings of National Academy of Sciences of the United States of America*, 99, 3318–3323. doi:10.1073/pnas.032675099
- Shera, C. A., & Zweig, G. (1993). Noninvasive measurement of the cochlear traveling-wave ratio. *Journal of the Acoustical Society of America*, 92, 1371–1381. doi:10.1121/1.405717
- Siegel, J. H. (1994). Ear-canal standing waves and high-frequency sound calibration using otoacoustic emission probes. *Journal of the Acoustical Society of America*, 95, 2589–2597. doi:10.1121/1.409829
- Sisto, R., & Moleti, A. (2007). Transient evoked otoacoustic emission latency and cochlear tuning at different stimulus levels. *Journal of the Acoustical Society of America*, 122, 2183–2190. doi:10.1121/1.2769981
- Sisto, R., Sanjust, F., & Moleti, A. (2013). Input/output functions of different-latency components of transient-evoked and stimulus-frequency otoacoustic emissions. *Journal of the Acoustical Society of America*, 133, 2240–2253. doi:10.1121/1.4794382
- Talmadge, C. L., Tubis, A., Long, G. R., & Piskorski, P. (1998). Modeling otoacoustic emission and hearing threshold fine structures. *Journal of the Acoustical Society of America*, 104, 1517–1543. doi:10.1121/1.424364
- Voss, S. E., Stenfelt, S., Neely, S. T., & Rosowski, J. J. (2013). Factors that introduce intrasubject variability into ear-canal absorbance measurements. *Ear and Hearing*, 34, 60S–64S. doi:10.1097/AUD.0b013e31829cfd64
- Wang X., Keefe D. H., & Gan R. Z. (2016). Predictions of middle-ear and passive cochlear mechanics using a finite element model of the pediatric ear. *Journal of the Acoustical Society of America*, 139, 1735–1746. doi:10.1121/1.4944949
- Zweig, G. (1976). Basilar membrane motion. In *Cold Spring Harbor symposia on quantitative biology* (Vol. XL, pp. 619–633). Cold Spring Harbor, NY: Cold Spring Harbor Laboratory. doi:10.1101/SQB.1976.040.01.058
- Zweig, G., & Shera, C. A. (1995). The origin of periodicity in the spectrum of evoked otoacoustic emissions. *Journal of the Acoustical Society of America*, 98, 2018–2047. doi:10.1121/1.413320